CZASOPISMO TECHNICZNE Ś
WYDAWNICTWO POLITECHNIKI KRAKOWSKIEJ

z. 3-Ś/2008
ISSN 0011-4561
ISSN 1897-6336

ADAM WOSATKO, JERZY PAMIN*, MARIA ANNA POLAK**,
ROMAN PUTANOWICZ*, ANDRZEJ WINNICKI***

SIMULATION OF FRACTURE IN RC SLAB–COLUMN CONNECTION STRENGTHENED AGAINST PUNCHING SHEAR

SYMULACJA PĘKANIA W ŻELBETOWYM POŁĄCZENIU PŁYTA–SŁUP WZMACNIANYM NA PRZEBICIE

Abstract

The paper presents a numerical analysis of an experimental slab-column configuration strengthened against punching shear. Two descriptions are used for concrete: gradient-enhanced isotropic elasticity-damage-plasticity and smeared fixed crack model. The elasto-plastic reinforcement is embedded in concrete. The results for both models are widely discussed.

Keywords: punching failure, slab-column connection, gradient damage, smeared cracks

Streszczenie

W artykule przedstawiono wyniki analizy numerycznej żelbetowego połączenia płyta-słup wzmacnianego na przebicie. Zastosowano dwa opisy betonu: gradientowy model izotropowej sprężysto-plastyczności sprzężonej z uszkodzeniem i model rozmazanych rys o stałym kierunku. Sprężysto-plastyczne zbrojenie zamodelowano bez poślizgu. Wyniki zostały szeroko omówione dla obu modeli.

Słowa kluczowe: zniszczenie przez przebicie, połączenie płyta-słup, gradientowa mechanika uszkodzeń, rysy rozmazane

*mgr Adam Wosatko, dr hab. Jerzy Pamin, dr Roman Putanowicz, Institute for Computational Civil Engineering, Faculty of Civil Engineering, Cracow University of Technology, Poland.
**prof. Maria Anna Polak, Department of Civil Engineering, University of Waterloo, Ontario, Canada.
***dr Andrzej Winnicki, Institute of Building Materials and Structures, Faculty of Civil Engineering, Cracow University of Technology, Poland.

1. Introduction

Slab-column structures are often designed in multi-storey and large-area buildings instead of traditional slab-girder-column combinations. Strengthening of reinforced concrete slabs against punching shear failure is then necessary. A new technique for the retrofit of existing slabs near slab-column connections has been developed and experimentally tested at the University of Waterloo [1]. In the experimens full-scale models representing interior slab-column connections were tested. The specimens were strengthened using a number of 9.5 mm bolts, symmetrically placed and anchored at both ends at slab surfaces. One slab had no shear bolts and served as a control specimen. It was found that the use of shear bolts increased the strength of the connection and significantly improved the ductility.

The problem of punching shear is difficult for simulation, since the interaction between flexural and shear failure needs to be reproduced, while localized fracture zones evolve. Some numerical simulations of punching shear are presented in [5, 8, 11]. Although the problem of proper simulation of localized failure is less severe in reinforced structures, the authors have decided to employ a regularized continuum description to minimize the effects of pathological mesh sensitivity and numerical instabilities.

In the paper the experiment is simulated using coupled isotropic elastic-damage-plastic relations for concrete and an elastic-plastic model for reinforcement, cf. [10] The model, formulated within linear kinematics and implemented in FEAP [9], includes a gradient localization limiter, cf. [3]. Two cases are considered: the slab without bolts and the slab with four bolts at each side of the column. Monotonically growing static loading is applied. The results of the computations and laboratory experiments are compared. Since the simulation results are not satisfactory for the model of the slab without bolts, the same configuration is computed with the classical smeared cracking model using the DIANA FE package [4].

2. Brief description of constitutive models

The main aim of the research is to simulate the laboratory test using a scalar damage-plasticity model for concrete, which includes a gradient localization limiter. The model, developed in [3], combines the gradient damage theory formulated in the strain space with the plasticity theory formulated in the space of effective stresses. In the former part of the model the modified von Mises loading function with exponential softening is used and in the latter the Burzyński-Drucker-Prager yield condition and linear hardening are assumed.

The theory involves an additional averaging equation which is responsible for regularization of the boundary value problem. In the employed three-dimensional two-field finite elements the averaged strain measure is discretized in addition to the displacements [7]. Consistently linearized numerical algorithms are employed.

For comparison the classical fixed crack model is used, in which the maximum principal tensile stress decides on the formation of a ‘crack’ smeared over a tributary area of a numerical integration point. Concrete in triaxial compression is assumed to be elastic, while the tensile cut-off is constant (Rankine cracking criterion). Exponential strain softening derived from the experiments of Hordijk [6] is assumed and constant shear retention is adopted. Secant stiffness option is used in equilibrium iterations in DIANA [4].

In both cases discrete embedded elastic-plastic reinforcement is modelled, i.e. no bond-slip between concrete and reinforcement is admitted.

3. Experimental data and results

In the experimental research [1] full-scale models representing interior slab-column connections were tested. The dimensions of the slabs were $1800 \times 1800 \times 120$ mm and the columns had square cross-section 150×150 mm. Simple supports were introduced at the bottom plane of the slab 150 mm from its edges. Additionally corners of the slab were clamped at the top against lifting. The specimens were loaded downwards through the column until failure. Note that the experimental configuration was in an upside down position in comparison with the real structural case. The flexural reinforcement was formed by bars of cross-section area $A_r = 100$ mm^2. The bars in the tension mat had the spacing of 100 mm and 90 mm for the upper and lower bar families, respectively, in order to produce almost identical bending capacities in the two orthogonal directions. The reinforcement bars at the compression side formed a grid with two times larger spacing. The column segments were reinforced with 4 bars having $A_r = 300$ mm^2.

One slab, called SB1, had no shear bolts installed and served as a control specimen. The other specimens were strengthened using an increasing number of symmetrically placed bolts with 9.5 mm diameter, at most four in each row, as in specimen SB4 shown in Fig. 1(b). The geometry and material properties from the experiment are shortly summarized in Table 1. The test results in terms of deflections, strains and crack widths were monitored. The experimental load-deflection diagrams for SB1 and SB4 are reproduced in this paper together with numerical results (cf. Fig. 3).

Table 1

Experimental data

Dimensions	mm	mm	mm
Slab	1800	1800	120
Column	150	150	
Supports	1500	1500	

Concrete strength	MPa
Tensile	2.13
Compress.	41

Reinforcement	Spacing mm	Cover mm	Sect. area mm	Yield strength MPa
In slab:				
Tensile	90/100	20	100	455
Compress.	200	20	100	455
In column:				
Bars			300	455
Ties			50	455
Bolts:				
First	45÷60		70.8	381
Subseq.	75÷90		70.8	381

The final experimental crack patterns for the selected slabs SB1 and SB4, as seen from the tension side, are presented in Fig. 1 (SB3 marked in the second photo is incorrect). For all examined specimens, the flexural cracks initiated at column corners and propagated radially

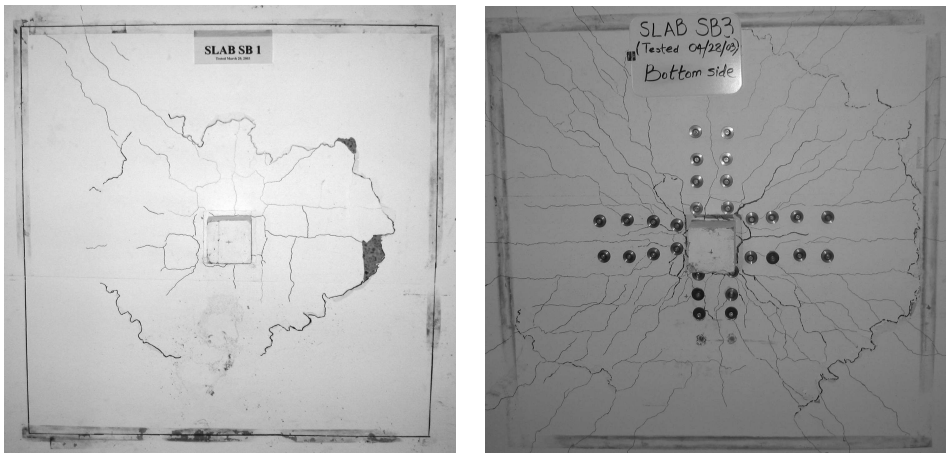

(a) (b)

Fig. 1. Final crack patterns for slabs SB1 and SB4, the tension side. Photos quoted from [1]. (a) Crack pattern for SB1, (b) crack pattern for SB4
Rys. 1. Końcowe formy zarysowania dla płyt SB1 i SB4, strona rozciągana. Zdjęcia przedrukowane z [1]. (a) Forma zarysowania – SB1, (b) forma zarysowania – SB4

towards the slab edges. It was found that specimen SB1 failed due to punching shear, but specimen SB4 failed in a flexural mode. The use of shear bolts increased the shear strength of the connection and significantly improved its ductility, see Fig. 3.

4. Simulation model and data

For the simulation a symmetric slab-column geometry and loading are selected, hence one quarter of the configuration is analyzed. In FEAP the slab and column are discretized with eight-noded two-field brick elements formulated as shown in [7], i.e. a linear interpolation of the displacements and averaged strain is used with full Gaussian integration. A top view on the applied mesh is presented in Fig. 2(a). Elasto-plastic truss elements are employed as the reinforcement (bond-slip between concrete and reinforcement is neglected). On the other hand, in DIANA standard eight-noded brick elements with selective integration of shear terms are used. The discrete reinforcement bars are embedded in the continuum elements.

In the numerical simulations the configuration is limited by support lines, i.e. a slab segment with dimensions $1500 \times 1500 \times 120$ mm is computed. Clamps are simulated by supporting three nodes near the corner of the slab. The distance between the tensile reinforcement truss elements is equal to 100 mm in both directions. The basic data for the computations are specified in Table 2. Two cases are considered in the simulations: the slab without bolts (SB1) and the slab with eight bolts at each side of the column (SB4), idealized using bar elements connected to the slab at its surfaces. The location of the whole reinforcement including optional bolts is depicted in Fig. 2(b). Static loading shown in Fig. 2(a) is applied under displacement control, i.e. the vertical movement of the upper plane of the column segment is imposed. The parameters for the gradient damage model are as follows:

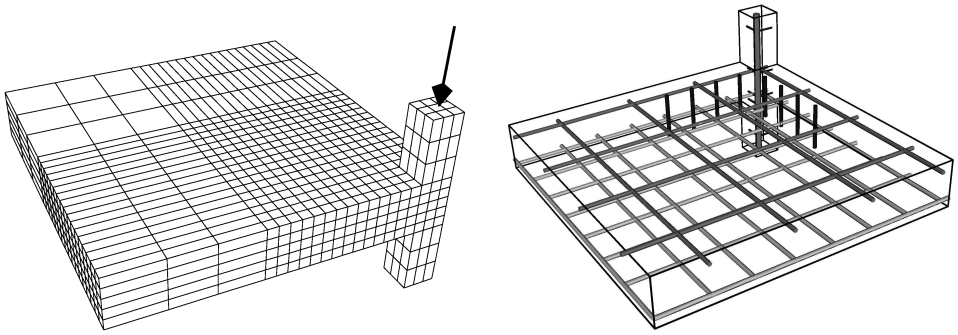

(a) (b)

Fig. 2. Simulated specimen. (a) Finite element mesh, (b) reinforcement in simulated specimen
Rys. 2. Definicja symulowanego obszaru. (a) Siatka MES, (b) wizualizacja zbrojenia

damage threshold $\kappa_0 = 6.2 \times 10^{-5}$, residual stress parameter $\alpha = 0.94$ and ductility parameter $\eta = 400$. In the basic case the ratio of compressive and tensile strength $k = f_c/f_t$ is equal to 20, which approximates the material data. In the simulation we combine this model with the Burzyński-Drucker-Prager hardening plasticity with weak coupling, i.e. the elastic strains induce damage [3]. The parameters for the plastic part of the model are: yield strength $\sigma_y = 2.13$ MPa, hardening modulus for cohesion $h_c = 17.2$ GPa, friction and dilatancy coefficients $\sin\phi = \sin\psi = 0.5$. The internal length scale is $l = 20$ mm which results in exaggerated smoothing and nonlocality, or $l = 4$ mm. The relation $c = \frac{1}{2}l^2$ is assumed to be valid [2] and the width of the fracture band is estimated as $w_f \approx 6l$. In order to mitigate the effect that cracking in the slab induces damage in the column due to nonlocality, which does

Table 2

Simulation data

Dimens.	mm	mm	mm
Slab	1500	1500	120
Column	150	150	
Supports	1500	1500	

Elastic constants	Young's modulus GPa	Poisson's ratio
Concrete	34.4	0.2
Steel	205	0.3

Concrete strength	MPa
Tensile, f_t	2.13
Compress.	$k \times f_t$

Reinforcement	Spacing mm	Cover (to axis) mm	Sect. area mm	Yield strength MPa
In slab:				
Tensile	100	24	100	455
Compress.	200	24	100	455
In column:				
Bars		25	300	455
Ties			50	455
Bolts:				
First	50		70.8	381
Subseq.	75		70.8	381

not seem to have a physical background, the behaviour of concrete elements in the column is constrained to be elastic.

In the cracking model in DIANA the fracture energy is $G_f = 106.5$ N/m, the estimated numerical crack bandwidth is $h = 24$ mm (smallest element size) and the shear retention factor $\beta = 0.2$.

5. Comparison of results

Figure 3 presents a comparison of experimental and computed diagrams. The initial response of the numerical model is too stiff. The load carrying capacity is well-represented for the model with bolts (experimental case SB4). This is not sufficient: it is not too difficult to tune the parameters of the damage-plasticity model to achieve this result. However, very similar results are obtained for the simulation *without* bolts (experimental case SB1). Actually the two diagrams in Fig. 3 can only be distinguished in the softening regime. This proves that the bolts are in fact hardly active in the numerical model which is in contradiction with the experimental results. The softening branch is simulated for $l = 20$ mm like in the experiment. This value of the internal length is quite large, the expected width of the fracture band is approximately $w_f = 120$ mm which is equal to the slab depth. The averaging and smoothing effect is then quite strong, the dissipated fracture energy strongly exaggerated, and for larger deflections damage is predicted in a large part of the slab, which is unrealistic.

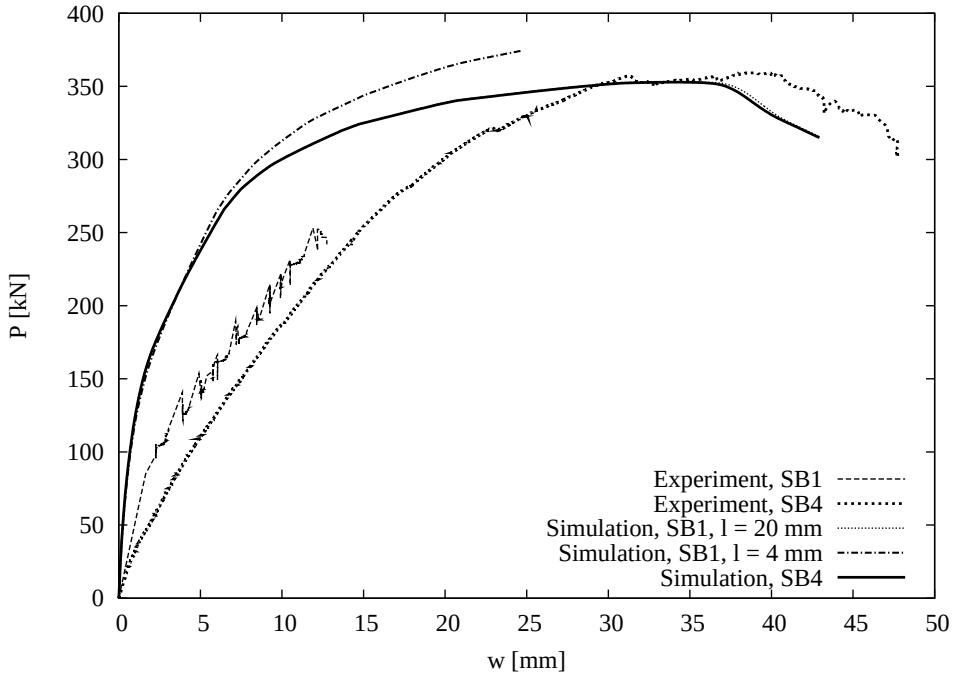

Fig. 3. Load-deflection diagrams for experiment and simulation in FEAP

Rys. 3. Wykresy siła-ugięcie z eksperymentu i symulacji wykonanej za pomocą FEAP-a

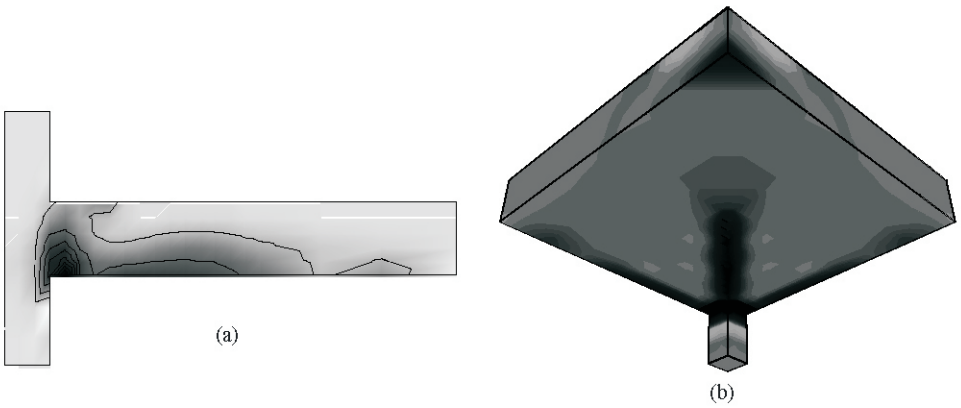

Fig. 4. Contour plots of averaged strain for damage-plasticity (implemented in FEAP), $k = 20$, $l = 20$ mm, with bolts, deflection w≈ 41 mm. (a) Side view, (b) bottom view
Rys. 4. Rysunki warstwicowe uśrednionego odkształcenia dla modelu mechaniki uszkodzeń i plastyczności (implementowanego w FEAP-ie), $k = 20$, $l = 20$ mm, ze sworzniami, ugięcie w≈ 41 mm. (a) Widok z boku, (b) widok od dołu

Therefore, in the second considered case a quite small value of the internal length parameter $l = 4$ mm is adopted. The related value $w_f = 24$ mm equals the element size in the dense mesh part, so this seems to be the limit value for the regularization to be active. The computations then fail at peak load and the higher stiffness and load-carrying capacity are attributed to the fact that the damaged zones are much less extensive.

Figure 4 presents the simulated averaged strain patterns for the former, basic case with the simulated bolts (thus representing the experimental case SB4). The contour plots represent the distributed cracking zones for three slab deflection values $w \approx 3, 12, 41$ mm. The plots are drawn for the cross section of the configuration with the vertical symmetry plane and for the bottom face of the slab, which exhibits tensile cracks. The figures show that a bending mode of failure is reproduced and the fracture first localizes in the direct vicinity of the column, then extending in zones following the symmetry planes of the configuration.

These results are close to the experimental behaviour for SB4, although the fracture patterns differ from experimental ones. However, the averaged strain patterns are similar for the case without bolts, which is unrealistic and shows that the model fails in predicting the punching shear phenomenon.

As can be seen in Fig. 4(a) the largest strains are finally observed at the bottom slab-column connection line. The tendency to predict that the slab will be cut directly at the column is observed also for other values of parameter $k = f_c/f_t$. In fact, the model is quite sensitive to the damage limit in compression, since the flexural failure mode is reproduced, cf. [10]. In particular, for $k = 10$ pronounced softening is predicted.

Figure 5 presents the averaged strain distributions for the small value of the internal length $l = 4$ mm and the case without bolts. Although the "crack" patterns at the bottom face of the slab are different from the case with $l = 20$ mm, no circular cracks are reproduced and the punching shear fracture along inclined cone-shaped surface at some distance from the column is not observed.

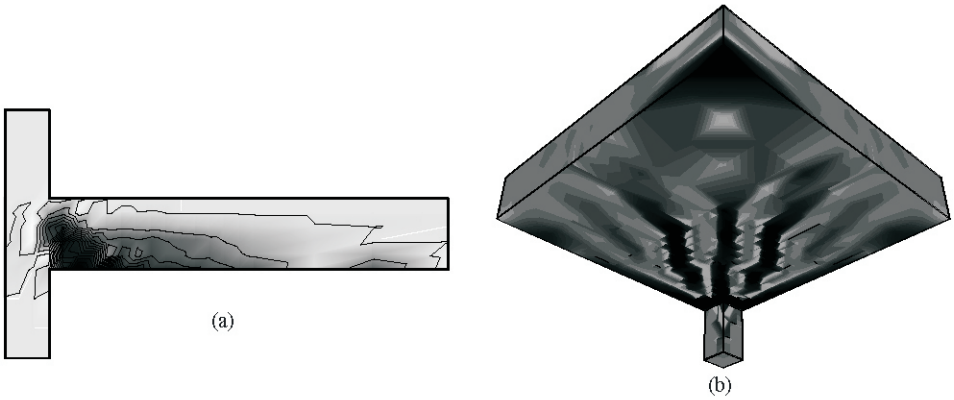

Fig. 5. Contour plots of averaged strain for damage-plasticity (implemented in FEAP), $k = 20$, $l = 4$ mm, with bolts, deflection w≈ 23 mm. (a) Side view, (b) bottom view
Rys. 5. Rysunki warstwicowe uśrednionego odkształcenia dla modelu mechaniki uszkodzeń i plastyczności (implementowanego w FEAP-ie), $k = 20$, $l = 4$ mm, ze sworzniami, ugięcie w≈ 23 mm. (a) Widok z boku, (b) widok od dołu

In both presented cases yielding of the flexural reinforcement is observed. Softening in the slab is so strong that it involves unloading in the reinforcement. However, the stresses in the retrofit bolts are rather small, they do not contribute much to the load carrying capacity during failure, since punching shear is not reproduced in the simulations.

Since a possible reason for the above-described incorrect simulation results could be that the nonlocal smoothing prevents the formation of secondary inclined fracture surface related

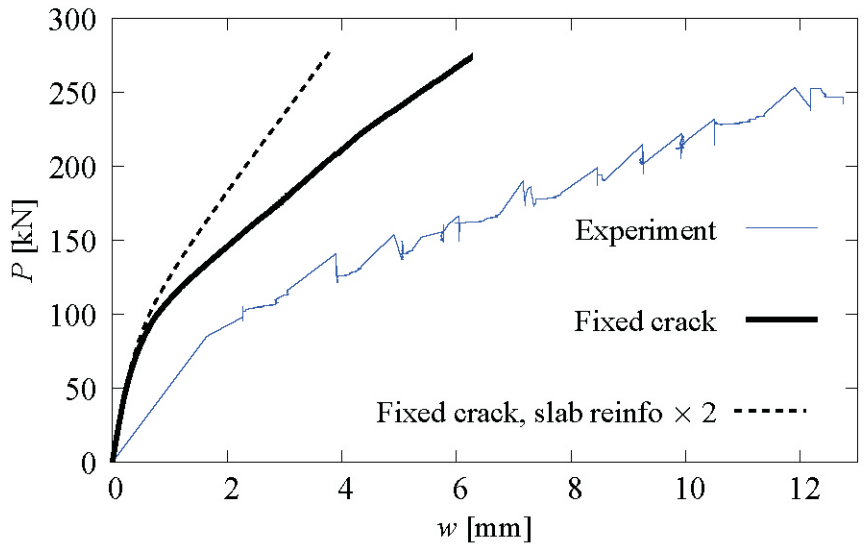

Fig. 6. Load-deflection diagrams obtained using DIANA package
Rys. 6. Wykresy siła-ugięcie otrzymane za pomocą pakietu DIANA

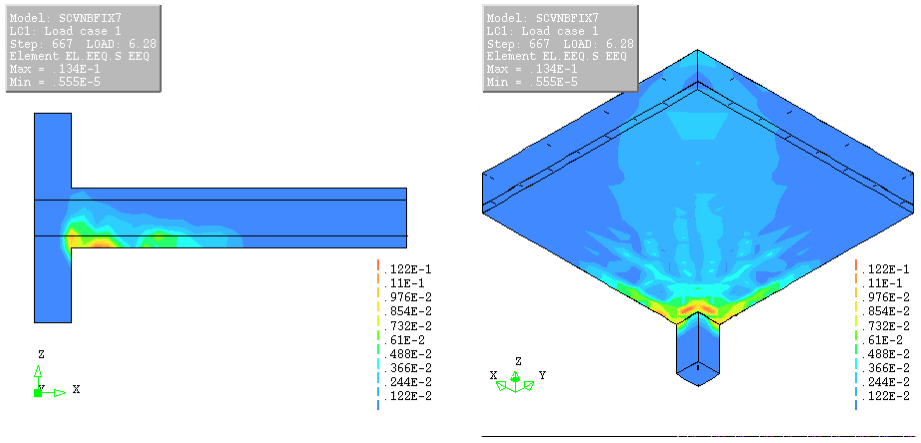

(a) (b)

Fig. 7. Contour plots of equivalent strain for model in DIANA, without bolts, deflection w≈ 6.2 mm. (a) Side view, (b) bottom view

Rys. 7. Rysunki warstwicowe odkształcenia równoważnego dla modelu w pakiecie DIANA, bez sworzni, ugięcie w≈ 6.2 mm. (a) Widok z boku, (b) widok od dołu

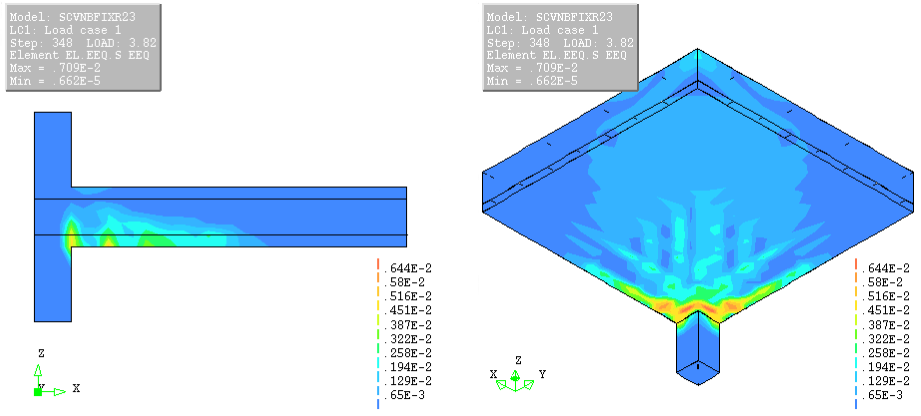

(a) (b)

Fig. 8. Contour plots of equivalent strain for model in DIANA, without bolts, double section area of tensile reinforcement in slab, deflection w≈ 3.8 mm. (a) Side view, (b) bottom view

Rys. 8. Rysunki warstwicowe odkształcenia równoważnego dla modelu w pakiecie DIANA, bez sworzni, z podwojonym polem przekroju zbrojenia rozciąganego w płycie, ugięcie w≈ 3.8 mm. (a) Widok z boku, (b) widok od dołu

to shear, the analysis of the configuration without the strengthening bolts has been repeated with the local fixed smeared crack model in the DIANA FE package. Figure 6 shows the load-deflection diagrams obtained for two considered cases: reinforcement according to Table 1 and double cross-section of the main reinforcement (in order to increase the flexural stiffness of the slab). It is noticed that in both cases failure of the simulation process is noticed at similar load value. For the actual reinforcement cross-section the happens soon after the bars yield in tension in the crack zone at the slab-column connection.

Figures 7 and 8 present the contour plots of the equivalent strain measure J_2^{ε} for the two respective cases, obtained right before the computations stop. Neither of the plots reproduces satisfactorily the punching shear failure mode, although secondary fracture zones develop at some distance from the column, which could initiate the shear cone as observed in the experiments if the iterative process did not fail. Moreover, the ductility of the model is insufficient.

6. Conclusions

The numerical simulations of fracture in the experimental slab-column configuration taken from [1] have not predicted the expected punching shear failure for the model without strengthening bolts. The results have neither been satisfactory for the gradient-enhanced elasticity-damage-plasticity model implemented by the authors in FEAP, nor for the classical fixed crack model from DIANA.

The former model reproduces the bending-type failure with yielding of the main reinforcement, which is consistent only with the experimental behaviour of the slab with bolts. On the other hand, it exhibits reasonable ductility and controlled localization. The latter model does not reproduce the shear failure either (shear cone is not observed), and fails for much smaller deflection.

References

[1] Adetifa B., Polak M.A., *Retrofit of interior slab-column connections for punching using shear bolts*, ACI Structural Journal, 102(2):268–274, 2005.

[2] Askes H., Pamin J., de Borst R., *Dispersion analysis and element-free Galerkin solutions of second- and fourth-order gradient-enhanced damage models*, Int. J. Numer. Meth. Engng, 49:811–832, 2000.

[3] de Borst R., Pamin J., Geers M.G.D., *On coupled gradient-dependent plasticity and damage theories with a view to localization analysis*, Eur. J. Mech. A/Solids, 18(6):939–962, 1999.

[4] DIANA, *DIANA Finite Element Analysis – User's manual, release 7.2*, Technical report, TNO Building and Construction Research, Delft 1999.

[5] Hallgren M., Bjerke M., *Non-linear element analyses of punching shear failure of column footings*, Cement & Concrete Composites, 24:491–496, 2002.

[6] Hordijk D.A., *Local approach to fatigue of concrete*, Ph.D. dissertation, Delft University of Technology, Delft 1991.

[7] Pamin J., Wosatko A., Winnicki A., *Two- and three-dimensional gradient damage-plasticity simulations of cracking in concrete*, N. Bićanić et al. (eds.) in: Proc. EURO-C 2003 Int. Conf. Computational Modelling of Concrete Structures, A.A. Balkema, Rotterdam/Brookfield 2003, 325–334.

[8] Polak M.A., *Modelling punching shear of reinforce concrete slabs using layered finite elements*, ACI Structural Journal, 95(1):71–80, 1998.

[9] Taylor R.L., *FEAP - A Finite Element Analysis Program, Version 7.4, User manual*, Technical report, University of California at Berkeley, Berkeley 2001.

[10] Wosatko A., Pamin J., Winnicki A., Putanowicz R., Polak M.A., *Numerical simulation of damage in reinforced concrete slab-column connection*, G. Meschke et al. (eds.) in: Proc. EURO-C 2006 Int. Conf. Computational Modelling of Concrete Structures, Taylor and Francis, London/Leiden 2006, 881–889.

[11] Xiao R.Y., O'Flaherty T., *Finite-element analysis of tested concrete connections*, Comput. & Struct., 78:247–255, 2000.